N94-14633

# Non-recursive Augmented Lagrangian Algorithms for the Forward and Inverse Dynamics of Constrained Flexible Multibodies

*Eduardo Bayo*

*Ragnar Ledesma*

Department of Mechanical Engineering
University of California
Santa Barbara, CA 93106

*ABSTRACT*

A technique is presented for solving the inverse dynamics of flexible planar multibody systems. This technique yields the non-causal joint efforts (inverse dynamics) as well as the internal states (inverse kinematics) that produce a prescribed nominal trajectory of the end effector. A non-recursive global Lagrangian approach is used in formulating the equations of motion as well as in solving the inverse dynamics equations. Contrary to the recursive method previously presented, the proposed method solves the inverse problem in a systematic and direct manner for both open-chain as well as closed-chain configurations. Numerical simulation shows that the proposed procedure provides an excellent tracking of the desired end effector trajectory.

## 1. Introduction

Accurate positioning and vibration minimization of flexible multibody systems have generated considerable interest from the computational dynamics and controls communities. The advent of the new generation of very fast, lightweight robots and flexible articulated space structures has made the control of structural vibrations an important practical problem in the manufacturing and space industries.

There is a large body of literature dealing with the forward dynamic analysis of flexible multibody systems, *i.e.*, determining the resulting motion when the joint forces and external forces are given. Numerous approaches have been proposed that are either based on the moving frame method or the inertial frame counterpart (see reference [1] and references therein.) Similarly, numerous control approaches have also been proposed for position and vibration control of flexible articulated structures (see reference [2] and references therein.)

Solutions to the non-collocated control of flexible articulated structures have been presented in [3-6]. The so-called inverse dynamics joint actuation are non-causal or time-delayed joint torques (applied in negative time and future time) that are capable of positioning the end effector according to a desired trajectory. The importance of using the inverse dynamics approach to vibration control has been demonstrated recently in reference [7] where passive feedback and feedforward of the inverse dynamics torque were used to achieve an exponentially stable tracking control law that yields excellent end-point tracking of flexible articulated structures. In this paper, present a global Lagrangian approach to the solution of vibration minimization and end-point trajectory tracking.

## 2. Mathematical Formulation

In order to describe the dynamic modeling let us consider a generic flexible body (Fig. 1) representing a component of a flexible articulated structure. The configuration of the multi-body system can be described by two sets of coordinates: the first set corresponds to the rigid body coordinates representing the location and orientation of the body axes, with respect to the inertial frame; and the second set corresponds to the so-called deformation coordinates or nodal deformations representing the deformation of the body with respect to the body axes. Using the aforementioned choice of coordinates, the location of an arbitrary point $P$ in a planar deformable body $i$ is given by

$$\mathbf{r}^i = \mathbf{R}^i + \mathbf{A}^i \, \mathbf{u}^i \tag{1}$$

where $\mathbf{R}^i$ is the location of the origin of the body axes with respect to the inertial frame, $\mathbf{u}^i$ is the location of point $P$ with respect to the body axes, and $\mathbf{A}^i$ is the rotation transformation matrix from the body axes to the inertial frame. In the three-dimensional case, the rotation transformation matrix is given by

$$\mathbf{A}^i = \begin{bmatrix} 2(\theta_0^2 + \theta_1^2) - 1 & 2(\theta_1\theta_2 - \theta_0\theta_3) & 2(\theta_1\theta_3 + \theta_0\theta_2) \\ 2(\theta_1\theta_2 + \theta_0\theta_3) & 2(\theta_0^2 + \theta_2^2) - 1 & 2(\theta_2\theta_3 - \theta_0\theta_1) \\ 2(\theta_1\theta_3 - \theta_0\theta_2) & 2(\theta_2\theta_3 + \theta_0\theta_1) & 2(\theta_0^2 + \theta_3^2) - 1 \end{bmatrix}^i \tag{2}$$

where the orientation coordinates are represented by four Euler parameters $\theta_0^i$, $\theta_1^i$, $\theta_2^i$, and $\theta_3^i$ which satisfy the following identity:

$$\sum_{k=0}^{3} (\theta_k^i)^2 = 1$$

The vector $\mathbf{u}^i$ can be decomposed into

$$\mathbf{u}^i = \mathbf{u}_r^i + \mathbf{u}_f^i \tag{3}$$

where $\mathbf{u}_r^i$ is the position vector of point $P$ in the undeformed state with respect to the body axes, and $\mathbf{u}_f^i$ is the deformation vector of point $P$ with respect to the body axes. Differentiating Eq. (1) with respect to time yields the velocity vector of point $P$

$$\dot{\mathbf{r}}^i = \dot{\mathbf{R}}^i + \dot{\mathbf{A}}^i \, \mathbf{u}^i + \mathbf{A}^i \, \dot{\mathbf{u}}_f^i \tag{4}$$

where $\dot{(\,)}$ represents differentiation with respect to time. To separate the generalized coordinates, the second term on the right hand side of Eq. (4) may be written as

$$\dot{\mathbf{A}}^i \, \mathbf{u}^i = -2 \, \mathbf{A}^i \, \tilde{\mathbf{u}}^i \, \mathbf{E}^i \, \dot{\boldsymbol{\theta}}^i \tag{5}$$

where $\mathbf{E}^i$ is a matrix that depends linearly on the Euler parameters and is given by

$$\mathbf{E}^i = \begin{bmatrix} -\theta_1 & \theta_0 & \theta_3 & -\theta_2 \\ -\theta_2 & -\theta_3 & \theta_0 & \theta_1 \\ -\theta_3 & \theta_2 & -\theta_1 & \theta_0 \end{bmatrix}^i \tag{6}$$

and $\tilde{\mathbf{u}}^i$ is a 3 x 3 skew-symmetric matrix given by

$$\tilde{\mathbf{u}}^i = \begin{bmatrix} 0 & -u_z & u_y \\ u_z & 0 & -u_x \\ -u_y & u_x & 0 \end{bmatrix}^i \tag{7}$$

where $u_x$, $u_y$, and $u_z$ are the coordinates of the generic point $P$ with respect to the body axes, in the deformed configuration.

The deformation vector $\mathbf{u}_f^i$ can be expressed in terms of the nodal deformations by using a finite element discretization scheme

$$\mathbf{u}_f^i = \mathbf{N}^i \, \mathbf{q}_f^i \tag{8}$$

where $\mathbf{N}^i$ is the shape function matrix and $\mathbf{q}_f^i$ is the nodal deformation vector. Since the shape function matrix is time-invariant, the time derivative of the deformation vector becomes

$$\dot{\mathbf{u}}_f^i = \mathbf{N}^i \, \dot{\mathbf{q}}_f^i \tag{9}$$

where $\dot{\mathbf{q}}_f^i$ is the time derivative of the vector of nodal deformations. Substituting Eqs. (5) and (9) into Eq. (4), we obtain the following expression for the velocity vector in terms of the rigid body coordinates and nodal deformation coordinates:

$$\dot{\mathbf{r}}^i = \dot{\mathbf{R}}^i - 2 \, \mathbf{A}^i \, \tilde{\mathbf{u}}^i \, \mathbf{E}^i \, \dot{\boldsymbol{\theta}}^i + \mathbf{A}^i \, \mathbf{N}^i \, \dot{\mathbf{q}}_f^i \tag{10}$$

Using Eq. (10) to describe the velocity vector of an arbitrary point $P$, the kinetic energy of body $i$ can be expressed in the following quadratic form in velocities

$$K.E.^i = \frac{1}{2} \left[ \dot{\mathbf{R}}^T \dot{\boldsymbol{\theta}}^T \dot{\mathbf{q}}_f^T \right]^i \begin{bmatrix} \mathbf{m}_{RR} & \mathbf{m}_{R\theta} & \mathbf{m}_{Rf} \\ \mathbf{m}_{\theta R} & m_{\theta\theta} & \mathbf{m}_{\theta f} \\ \mathbf{m}_{fR} & \mathbf{m}_{f\theta} & \mathbf{m}_{ff} \end{bmatrix}^i \begin{bmatrix} \dot{\mathbf{R}} \\ \dot{\boldsymbol{\theta}} \\ \dot{\mathbf{q}}_f \end{bmatrix}^i \tag{11}$$

where the constant submatrices $\mathbf{m}_{RR}$ and $\mathbf{m}_{ff}$ represent the total mass of the body and the consistent finite element mass matrix, respectively. The submatrix $m_{\theta\theta}$ represents the moment of inertia of the deformable body about the origin of the body axes, and the submatrix $\mathbf{m}_{\theta R}$ represents the first moment of mass of the deformable body about the body axes. The submatrices $\mathbf{m}_{fR}$ and $\mathbf{m}_{f\theta}$ represent the kinematic coupling between the rigid body coordinates and the nodal deformation coordinates.

The potential energy due to linear elastic strains in the material can be expressed in the following quadratic form in rigid body coordinates and nodal deformation coordinates

$$P.E.^i = \frac{1}{2} \left[ \mathbf{R}^T \boldsymbol{\theta}^T \mathbf{q}_f^T \right]^i \begin{bmatrix} 0 & 0 & 0 \\ 0 & 0 & 0 \\ 0 & 0 & \mathbf{k}_{ff} \end{bmatrix}^i \begin{bmatrix} \mathbf{R} \\ \boldsymbol{\theta} \\ \mathbf{q}_f \end{bmatrix}^i \tag{12}$$

where $\mathbf{k}_{ff}$ is the conventional finite element stiffness matrix. The singularity of the stiffness matrix can be eliminated by imposing appropriate boundary conditions or by choosing vibration modes that are consistent with the boundary conditions.

### 2.1. Equations of Motion

In order to unify the equations formulated in rigid body dynamics and structural dynamics, we make use of generalized coordinates which include rigid body coordinates and deformation coordinates, hence

$$\mathbf{q}^i = \begin{bmatrix} \mathbf{R} \\ \boldsymbol{\theta} \\ \mathbf{q}_f \end{bmatrix}^i = \begin{bmatrix} \mathbf{q}_r \\ \mathbf{q}_f \end{bmatrix}^i \tag{13}$$

where $\mathbf{q}^i$ is the vector of generalized coordinates for body $i$, $\mathbf{q}_r^i$ and $\mathbf{q}_f^i$ are the rigid body coordinates and nodal deformation coordinates of body $i$, respectively. The kinetic energy of the body can therefore be expressed by

$$K.E.^i = \frac{1}{2}\,\dot{\mathbf{q}}^{iT}\,\mathbf{M}^i\,\dot{\mathbf{q}}^i \tag{14}$$

where $\mathbf{M}^i$ is the overall mass matrix of body $i$. Similarly, the potential energy of the body due to linear elastic deformation can be expressed by

$$P.E.^i = \frac{1}{2}\,\mathbf{q}^{iT}\,\mathbf{K}^i\,\mathbf{q}^i \tag{15}$$

where $\mathbf{K}^i$ is the overall stiffness matrix of body $i$.

When reference coordinates such as those described in this paper are employed in multibody systems, the generalized coordinates are not independent because the motion of specific points in different bodies are related according to the type of mechanical joint that connects the contiguous bodies. Moreover, in flexible mechanical systems, the deformation of a component affects the configuration of adjacent components. The interdependence of the generalized coordinates are expressed by a vector of kinematic constraint equations, such as

$$\boldsymbol{\Phi}(\mathbf{q},t) = 0 \tag{16}$$

where $\mathbf{q}$ is the total vector of system generalized coordinates, $t$ is time, and $\boldsymbol{\Phi}$ is the vector of linearly independent holonomic constraint equations. For example, if a revolute joint connects two flexible planar bodies $i$ and $j$ at points $P$ and $Q$ shown in Fig. 2, two constraint equations corresponding to the constraint condition that requires points $P$ and $Q$ to be coincident can be written as

$$\left[\mathbf{R}^i + \mathbf{A}^i\,\mathbf{u}_P^i\right] - \left[\mathbf{R}^j + \mathbf{A}^j\,\mathbf{u}_Q^j\right] = 0 \tag{17}$$

In general, holonomic constraints can also be explicit functions of time as well as generalized coordinates, as in the case of imposing the coordinates of the end-effector to follow a desired trajectory.

Using Lagrange's equations for a system with constrained coordinates, the system equations of motion will take the form

$$\mathbf{M}(\mathbf{q})\,\ddot{\mathbf{q}} + \mathbf{C}\,\dot{\mathbf{q}} + \mathbf{K}\,\mathbf{q} + \boldsymbol{\Phi}_\mathbf{q}^{\mathrm{T}}\,\boldsymbol{\lambda} = \mathbf{Q}_\mathbf{e} + \mathbf{Q}_\mathbf{v}(\mathbf{q},\dot{\mathbf{q}}) \tag{18}$$

where $\mathbf{M}$, $\mathbf{C}$ and $\mathbf{K}$ are the system mass, system damping and system stiffness matrices, respectively, $\boldsymbol{\lambda}$ is the vector of Lagrange multipliers associated with the constraints, $\boldsymbol{\Phi}_\mathbf{q}$ is the constraint Jacobian matrix, $\mathbf{Q}_\mathbf{e}$ is the vector of applied external forces, and $\mathbf{Q}_\mathbf{v}$ is the quadratic velocity vector. The quadratic velocity vector contains the centrifugal forces and Coriolis forces that result from the differentiation of the kinetic energy expression with respect to the generalized coordinates.

In a forward dynamic analysis, *i.e.*, finding the resulting motion given the applied joint forces and external forces, Eqs. (16) and (18) form a mixed system of differential-algebraic equations (DAE's) that have to be solved simultaneously. The solution to the inverse dynamics problem requires a forward dynamic analysis within an iteration process. We solve the forward dynamics problem by using the augmented Lagrangian penalty formulation [8]. The augmented Lagrangian penalty formulation obviates the need to solve a mixed set of differential-

algebraic equations and does not increase the number of equations to account for the constraints. Applying the augmented Lagrangian penalty formulation to Eqs. (16) and (18) will result in the following equation:

$$M(q)\,\ddot{q} + C\,q + K\,q + \Phi_q^T\,\alpha\left[\ddot{\Phi} + 2\,\mu\,\omega\,\dot{\Phi} + \omega^2\,\Phi\right] = Q_e + Q_v(\dot{q},q) - \Phi_q^T\,\lambda^* \qquad (19)$$

where $\alpha$ is a diagonal matrix of penalty factors whose elements are large real numbers that will assure the satisfaction of constraints, $\omega$ and $\mu$ are diagonal matrices representing the natural frequencies and damping characteristics of the dynamic penalty system associated with the constraints. The augmented Lagrangian method requires an iteration for the correct value of the Lagrange multipliers. The recursive equation for the Lagrange multipliers is given by

$$\lambda_{i+1}^* = \lambda_i^* + \alpha\left[\ddot{\Phi} + 2\,\mu\,\omega\,\dot{\Phi} + \omega^2\,\Phi\right] \qquad (20)$$

## 2.2. Inverse Kinematics and Inverse Dynamics

In the context of end-point motion and vibration control, the inverse dynamics refers to the problem of finding the actuating forces or torques that will cause the end-point of a flexible articulated structure to follow a desired trajectory. The study done in reference [9] showed that because of the non-minimum phase character of the inverse problem, the stable solution has to be non-causal, *i.e.*, actuation is required before the end-point has started to move as well as after the the end-point has stopped. In this paper, we use a global Lagrangian approach to solve the planar inverse dynamics problem. The equations of motion are partitioned to yield explicit expressions for the joint actuations and linearized elastic equations of motion that are readily suitable for non-causal inversion.

In partitioned form, Eq. (18) can be written as

$$\begin{bmatrix} m_{RR} & m_{R\theta} & m_{Rf} \\ m_{\theta R} & m_{\theta\theta} & m_{\theta f} \\ m_{fR} & m_{f\theta} & m_{ff} \end{bmatrix} \begin{bmatrix} \ddot{R} \\ \ddot{\theta} \\ \ddot{q}_f \end{bmatrix} + \begin{bmatrix} 0 & 0 & 0 \\ 0 & 0 & 0 \\ 0 & 0 & c_{ff} \end{bmatrix} \begin{bmatrix} \dot{R} \\ \dot{\theta} \\ \dot{q}_f \end{bmatrix} + \begin{bmatrix} 0 & 0 & 0 \\ 0 & 0 & 0 \\ 0 & 0 & k_{ff} \end{bmatrix} \begin{bmatrix} R \\ \theta \\ q_f \end{bmatrix} + \begin{bmatrix} \Phi_R^T \\ \Phi_\theta^T \\ \Phi_{q_f}^T \end{bmatrix} \lambda = \begin{bmatrix} Q_{eR} \\ Q_{e\theta} \\ Q_{ef} \end{bmatrix} + \begin{bmatrix} Q_{vR} \\ Q_{v\theta} \\ Q_{vf} \end{bmatrix} \qquad (21)$$

The second set of equations in Eq. (21) can be rearranged to express the externally applied joint forces as

$$Q_{e\theta} = m_{\theta R}\,\ddot{R} + m_{\theta\theta}\,\ddot{\theta} + m_{\theta f}\,\ddot{q}_f + \Phi_\theta^T\,\lambda - Q_{v\theta} \qquad (22)$$

Eq. (22) is the inverse dynamics equation that yields the joint forces (torques) necessary for the end-point to follow a prescribed trajectory. In order to obtain $Q_{e\theta}$, the nodal acceleration vector $\ddot{q}_f$ is needed. This vector can be obtained from the third set of equations in Eq. (21), which can be written as

$$m_{ff}\,\ddot{q}_f + c_{ff}\,\dot{q}_f + k_{ff}\,q_f = Q_{ef} + Q_{vf} - \Phi_{q_f}^T\,\lambda - m_{fR}\,\ddot{R} - m_{f\theta}\,\ddot{\theta} \qquad (23)$$

The linearized form of Eq. (23) makes the nonlinear inversion problem amenable to successive linear inversion techniques. The vector of applied nodal forces $Q_{ef}$ can be expressed in terms of the externally applied torques through the following mapping:

$$Q_{ef} = G_f\,Q_{e\theta} \qquad (24)$$

where in the planar case, the matrix $G_f$ is a constant matrix which maps the externally applied torques to the vector of externally applied nodal forces. Substituting Eqs. (22) and (24) into

Eq. (23) results in

$$\mathbf{m}_{ff}\,\ddot{\mathbf{q}}_f + \mathbf{c}_{ff}\,\dot{\mathbf{q}}_f + \mathbf{k}_{ff}\,\mathbf{q}_f = \mathbf{G}_f\,\mathbf{m}_{\theta f}\,\ddot{\mathbf{q}}_f + \mathbf{F}_1(\boldsymbol{\lambda},\mathbf{q}_r,\dot{\mathbf{q}}_r,\ddot{\mathbf{q}}_r,\mathbf{q}_f,\dot{\mathbf{q}}_f) \tag{25}$$

where $\mathbf{F}_1$ is a force vector that includes the inertial terms, reaction terms between contiguous bodies, and quadratic velocity terms.

The inertial coupling submatrix $\mathbf{m}_{\theta f}$ can be decomposed into a sum of a time-invariant matrix and a time-varying matrix

$$\mathbf{m}_{\theta f} = \mathbf{m}^c_{\theta f} + \mathbf{m}^t_{\theta f} \tag{26}$$

where $\mathbf{m}^c_{\theta f}$ and $\mathbf{m}^t_{\theta f}$ are the time-invariant part and time-varying part of $\mathbf{m}_{\theta f}$, respectively. This decomposition is essential for the iteration process needed to obtain the solution as explained below. Substituting Eq. (26) into Eq. (25), we obtain the inverse kinematics equation of motion for the nodal displacements $\mathbf{q}_f$:

$$\mathbf{m}^*_{ff}\,\ddot{\mathbf{q}}_f + \mathbf{c}_{ff}\,\dot{\mathbf{q}}_f + \mathbf{k}_{ff}\,\mathbf{q}_f = \mathbf{F}(\boldsymbol{\lambda},\mathbf{q}_r,\dot{\mathbf{q}}_r,\ddot{\mathbf{q}}_r,\mathbf{q}_f,\dot{\mathbf{q}}_f,\ddot{\mathbf{q}}_f) \tag{27}$$

where

$$\mathbf{m}^*_{ff} = \mathbf{m}_{ff} - \mathbf{G}_f\,\mathbf{m}^c_{\theta f} \tag{28}$$

The problem statement for the inverse kinematics is that of finding the internal states $\mathbf{q}_f$ so that the end-point coordinates characterized by a subset of the rigid body coordinates $\mathbf{q}_r$ follow a prescribed trajectory. The mass matrix $\mathbf{m}^*_{ff}$ is nonsymmetric and it is precisely the nonsymmetry of the mass matrix that produces internal states which are non-causal with respect to the end-point motion. Eq. (27) is a nonlinear differential equation in the variable $\mathbf{q}_f$. As explained below, Eq. (27) is solved iteratively in the frequency domain to yield the nodal deformation vector $\mathbf{q}_f$ that is non-causal with respect to the end-point motion.

In the frequency domain, Eq. (27) can be written as a set of complex equations for a particular frequency $\bar{\omega}$

$$\left[\mathbf{m}^*_{ff} + \frac{1}{i\bar{\omega}}\,\mathbf{c}_{ff} - \frac{1}{\bar{\omega}^2}\,\mathbf{k}_{ff}\right]\hat{\ddot{\mathbf{q}}}_f(\bar{\omega}) = \hat{\mathbf{F}}(\bar{\omega}) \tag{29}$$

where $\hat{\ddot{\mathbf{q}}}_f(\bar{\omega})$ is the Fourier transform of $\ddot{\mathbf{q}}_f(t)$ and $\hat{\mathbf{F}}(\bar{\omega})$ is the Fourier transform of $\mathbf{F}(t)$. Eq. (29) is based on the assumption that $\ddot{\mathbf{q}}_f(t)$ and $\mathbf{F}(t)$ are Fourier transformable. This assumption is valid for slewing motions which are from rest to rest. The nodal acceleration vector $\ddot{\mathbf{q}}_f(\bar{\omega})$ can be obtained directly from Eq. (29) for each frequency $\bar{\omega}$. The leading matrix of Eq. (29) is a complex regular matrix that is invertible for all frequencies except for $\bar{\omega} = 0$. However, for $\bar{\omega} = 0$, the system undergoes a rigid body motion determined only by the invertible mass matrix $\mathbf{m}^*_{ff}$. The nodal accelerations in the time domain may be obtained through the application of the inverse Fourier transform, *i.e.*,

$$\ddot{\mathbf{q}}_f(t) = \frac{1}{2\pi}\int_{-\infty}^{\infty}\hat{\ddot{\mathbf{q}}}_f(\bar{\omega})\,e^{i\bar{\omega}t}\,d\bar{\omega} \tag{30}$$

Once the non-causal nodal accelerations are known, Eq. (22) can be used to explicitly compute the non-causal inverse dynamics joint efforts that will move the end effector according to a desired trajectory. We note, however, that the inverse dynamics torque and internal

states given by Eqs. (22) and (27), respectively, depend on the Lagrange multipliers and rigid body coordinates, which in turn depend on the internal states and the applied torque. Moreover, the rigid body coordinates and Lagrange multipliers are different from their nominal values when the components of the multibody system are flexible. Therefore, a forward dynamic analysis is required to obtain an improved estimate of the generalized coordinates and Lagrange multipliers given the torques computed previously using nominal values of rigid body coordinates and Lagrange multipliers. In order to ensure that the iteration process converges to obtain the joint efforts that will cause the end-effector to follow the desired trajectory, the forward dynamics analysis is carried out with the additional constraint that the coordinates of the end-point follow the desired trajectory. These additional constraints have corresponding Lagrange multipliers which act as correcting terms to the joint efforts that have been previously calculated.

To summarize, the procedure for obtaining the inverse dynamics solution for flexible multibody systems involve the following steps:

**Algorithm:**

1. Perform a rigid body inverse dynamic analysis to obtain the nominal values of the rigid body coordinates $\mathbf{q}_r$ and Lagrange multipliers $\boldsymbol{\lambda}$.
2. Solve the inverse kinematics equation represented by Eq. (27) to obtain the time-delayed nodal accelerations $\ddot{\mathbf{q}}_f$.
3. Compute the inverse dynamics joint efforts $\mathbf{Q}_{e\theta}$ using Eq. (22).
4. Perform a forward dynamic analysis using Eq. (19) to obtain new values for the generalized coordinates and Lagrange multipliers.
5. Repeat steps 2 through 4 until convergence in the inverse dynamics torques is achieved.

## 3. Simulation Results

We present in this section the results of numerical simulations that verify the procedure discussed above. First, we apply the global Lagrangian approach to an open-chain flexible multibody system and compare the results with those obtained by the recursive Newton-Euler method [5] to test the validity of the proposed procedure. Next, we present the results of the application of the global Lagrangian approach to a closed-chain flexible multibody system to determine the inverse dynamics torque that will produce the desired motion at the end effector.

### 3.1. Open-Chain Multibody System

Fig. 3 shows a two-link flexible multibody system in the horizontal plane. The end-point of the second link is specified to move along the x-axis according to the acceleration profile described by Fig. 5, which corresponds to an end-point displacement of 0.483 meters along the x-axis. The geometric and material properties of the links are:

First Link:

Length: 0.66 $m$
Cross-section area: $1.2 \times 10^{-4}\ m^2$
Cross-section moment of inertia: $2.3 \times 10^{-10}\ m^4$

Second Link:

Length: $0.66m$
Cross-section area: $4.0 \times 10^{-5}\ m^2$
Cross-section moment of inertia: $8.5 \times 10^{-12}\ m^4$

The two links share the following properties:

Young's modulus: 14 $GPa$
Mass density: $2715\ kg/m^3$

In Fig. 6, the inverse dynamics torque profile for the base motor using the global Lagrangian method is superimposed on the inverse dynamics torque profile determined by the recursive Newton-Euler method. The inverse dynamics torque profiles for the elbow motor computed by the two aforementioned methods are superimposed in Fig. 7. Both the recursive and global formulations yield the same result and superimpose to each other, thus validating the proposed method. The corresponding rigid body torques are also shown in Figs. 6 and 7 to illustrate the pre-actuation and post-actuation present in the inverse dynamics torque profiles.

### 3.2. Closed-Chain Multibody System

Fig. 4 shows a closed-chain flexible multibody system made up of four flexible links with two joints which are fixed against translation relative to the ground. As in the open-chain case, the multibody system is assumed to lie on a horizontal plane so that gravity effects are neglected. The desired trajectory of joint 5 is a straight line 45 degrees with respect to the x and y axes. The x and y-components of the acceleration of joint 5 are specified to follow the acceleration profile shown in Fig. 8. The four links share the following geometric and material properties:

Length: 0.60 $m$
Cross-section area: $4.0 \times 10^{-5}\ m^2$
Cross-section moment of inertia: $8.5 \times 10^{-12}\ m^4$
Young's modulus: 14 $GPa$
Mass density: $2715\ kg/m^3$

Fig. 9 shows the inverse dynamics torque profile at joint 1 obtained by the global Lagrangian method. The rigid body inverse dynamics torque profile is superimposed for comparison. The figure shows the noncausal character of the solution for the inverse problem. Fig. 10 shows the inverse dynamic torque profile at joint 3 superimposed with the corresponding rigid body inverse dynamics torque profile. Again, the time delay due to the noncausality of the solution is seen in this figure.

Fig. 11 shows the elastic angular rotation at the base of the first link obtained by a feedforward of the inverse dynamics torque. Superimposed in the same figure is the corresponding elastic angular rotation obtained by a feedforward of the rigid body torque. Whereas the rigid body torque produces residual angular rotations, the inverse dynamic torque does not show

residual angular rotations. As a matter of fact, it has been observed in the simulations that the rigid body torques produced residual vibration in all the nodal deformations while the inverse dynamics torques eliminated the residual oscillation. Furthermore, the inverse dynamics torques produced nodal deformations which exhibit non-causal characteristics with respect to the end-point motion. Fig. 12 shows a comparison of the vertical tip error at joint 5 obtained by a feedforward of the inverse dynamics torque with the tip error resulting from a feedforward of the rigid body torque. This figure shows that the inverse dynamics torque provides an excellent tracking of the desired end effector trajectory whereas the rigid body torque again induces substantial vibration on the end-point motion.

## 4. Conclusion

A global Lagrangian approach for the inverse dynamics of flexible multibody systems has been presented. The procedure is capable of solving for the inverse dynamics torque profiles of both open-chain and closed-chain flexible multibody systems in a unified and systematic manner. The method is found to produce an excellent tracking of the desired trajectory of the end effector. In a future paper, we will address the inverse dynamics problem for flexible multibody systems undergoing motion in three dimensions. New problems arise in the three-dimensional case, since the actuating torque vectors have directions which are time-varying and nonlinear functions of the rigid body coordinates, as contrasted with the planar case where the applied torque vectors have directions fixed perpendicular to the plane of the multibody system. In addition, to be able to perform the inverse kinematics and inverse dynamics analyses, additional actuation at the joints may be necessary.


### Acknowledgements

The support of this work by the Air Force Office of Scientific Research under contract no. F49620-91-C-0095 and by TRW is gratefully acknowledged.


### References


1. A. A. Shabana, *Dynamics of Multibody Systems*, John Wiley & Sons, Inc., 1989.
2. M. C. Oakley and R. H. Cannon, "Anatomy of an experimental two-link flexible manipulator under end-point control," *Proceedings, 29th IEEE Conference on Decision and Control*, Honolulu, Hawaii, December 1990.
3. E. Bayo, "A finite-element approach to control the end-point motion of a single-link flexible robot," *Journal of Robotic Systems*, vol. 4, no. 1, pp. 63-75, 1987.
4. E. Bayo and H. Moulin, "An efficient computation of the inverse dynamics of flexible manipulators in the time domain," *Proceedings, IEEE Conference on Robotics and Automation*, pp. 710-715, 1989.
5. E. Bayo, P. Papadopoulos, J. Stubbe and M. Serna, "Inverse kinematics and dynamics of a multi-link elastic robot: an iterative frequency domain," *International Journal of Robotics Research*, vol. 8, no. 6, pp. 49-62, 1989.
6. D. S. Kwon and W. J. Book, "An inverse dynamic method yielding flexible manipulator state trajectories," *Proceedings, American Control Conference* , San Diego, California, 1990.

7. B. Paden, D. Chen, R. Ledesma and E. Bayo, "Exponentially stable tracking control for multi-joint flexible-link manipulators," *ASME Journal of Dynamic Systems, Measurement and Control.* Accepted for publication.

8. E. Bayo, J. Garcia de Jalon and M. Serna, "A modified lagrangian formulation for the dynamic analysis of constrained mechanical systems," *Computer Methods in Applied Mechanics and Engineering*, vol. 71, pp. 183-195, Nov. 1988.

9. H. Moulin, "Problems in the inverse dynamics solution for flexible manipulators," *Ph.D. Thesis*, University of California, Santa Barbara, 1989.

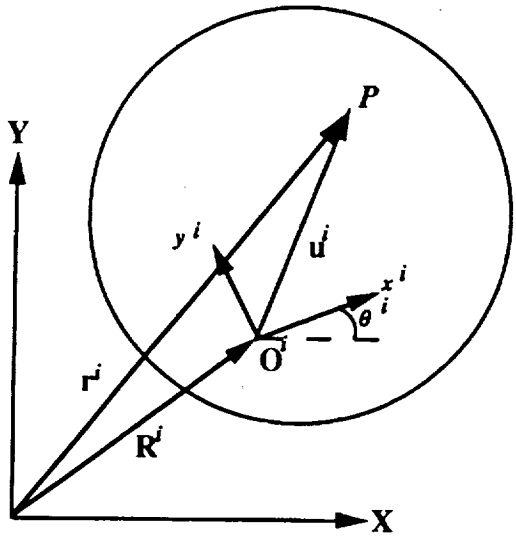


Fig. 1: Reference coordinates for planar body i

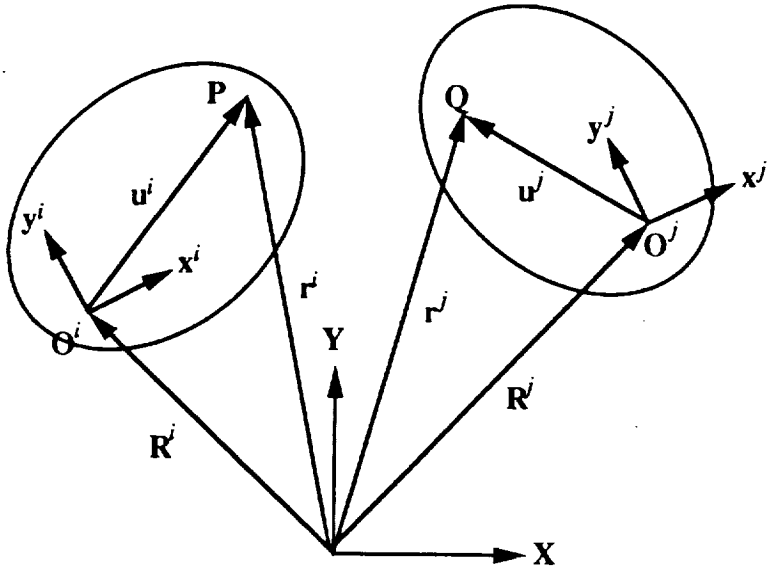


Fig. 2: A pair of flexible planar bodies

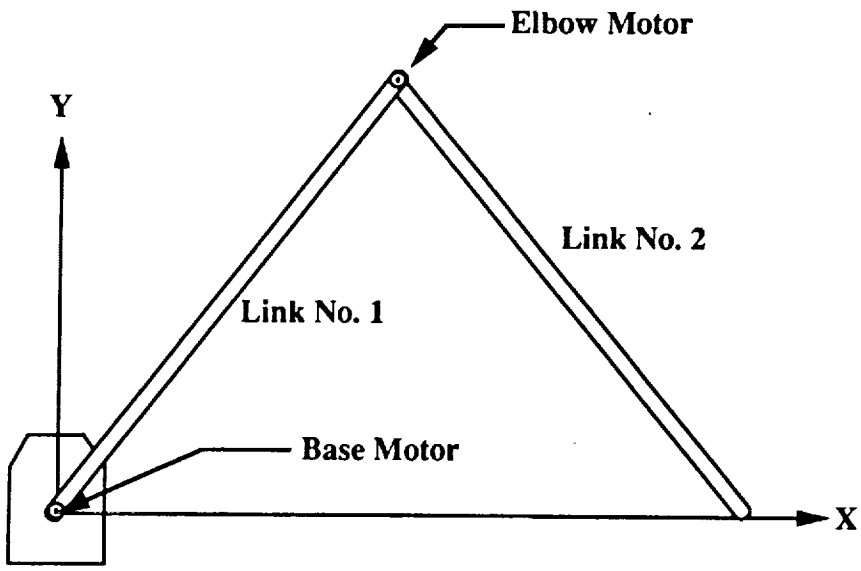


Fig. 3: Two-Link Open-Chain Flexible Multibody System

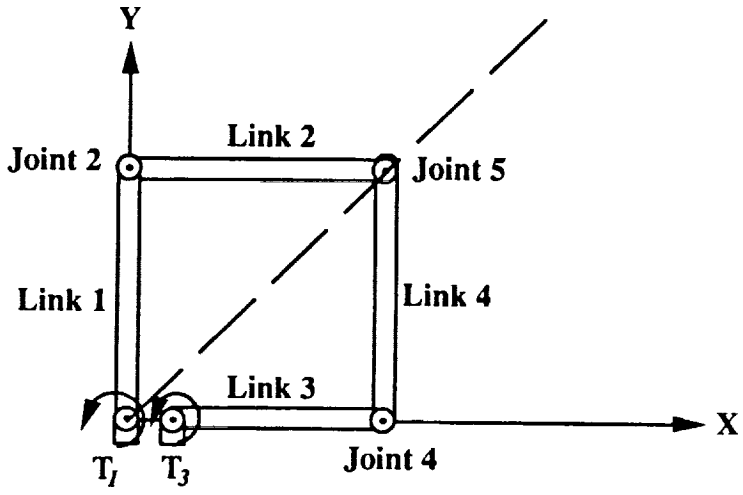


Fig.4: Closed-Chain Flexible Multibody System

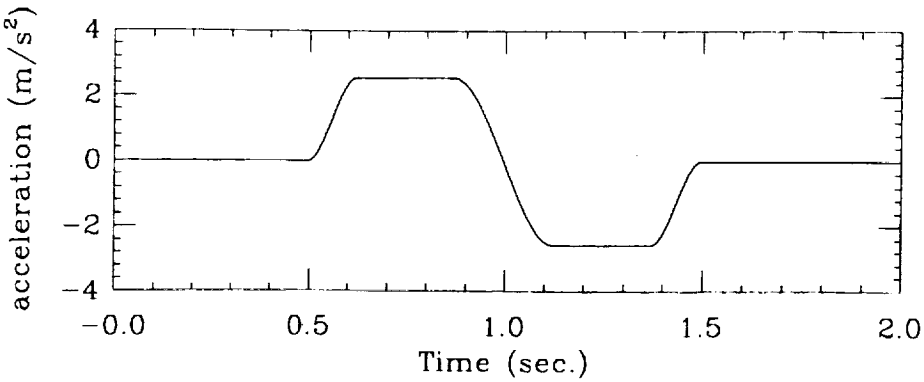


Fig. 5: end−point acceleration along the x−axis

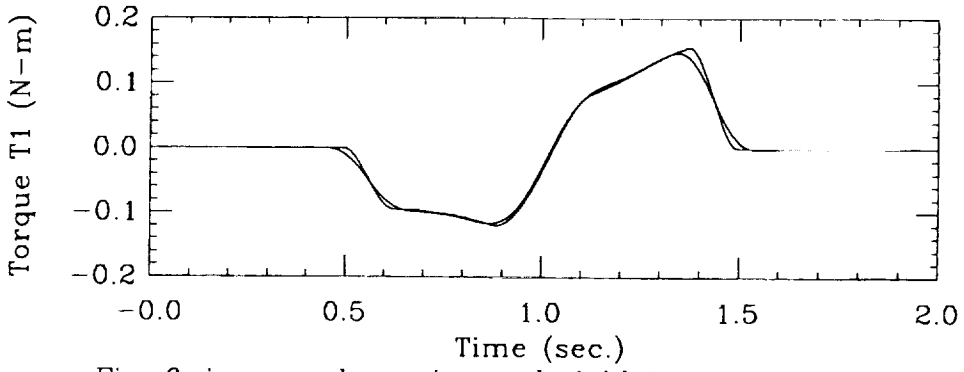


Fig. 6: inverse dynamics and rigid torque at base motor

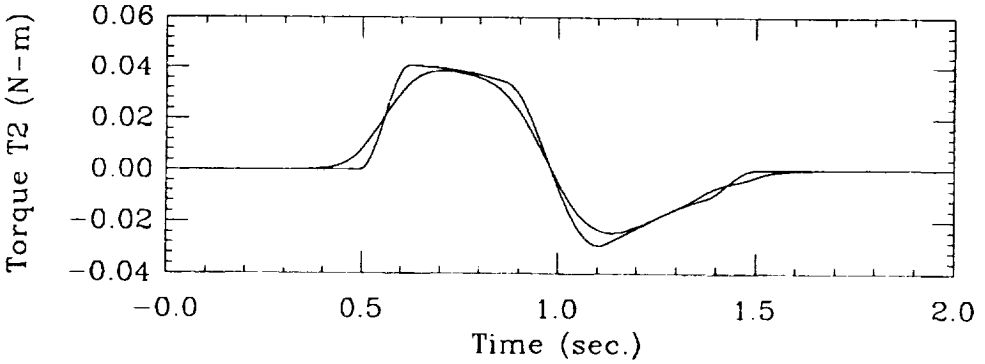


Fig. 7: inverse dynamics and rigid torque at elbow motor

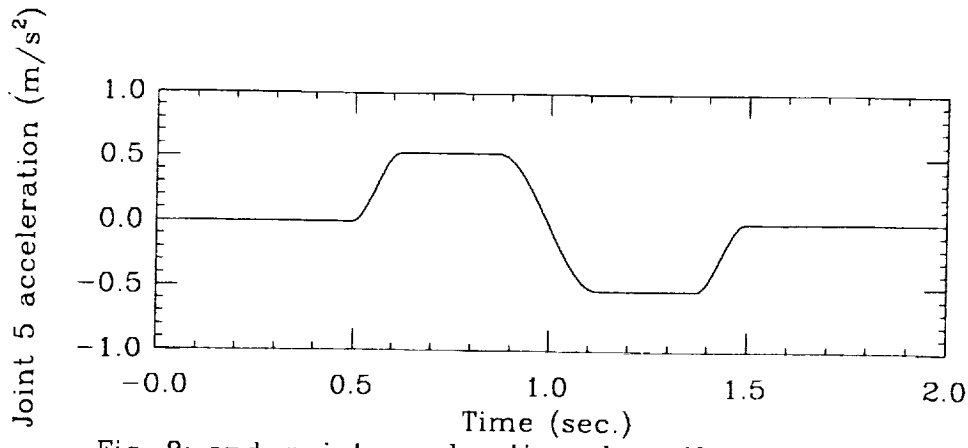


Fig. 8: end−point acceleration along the x− and y− axes

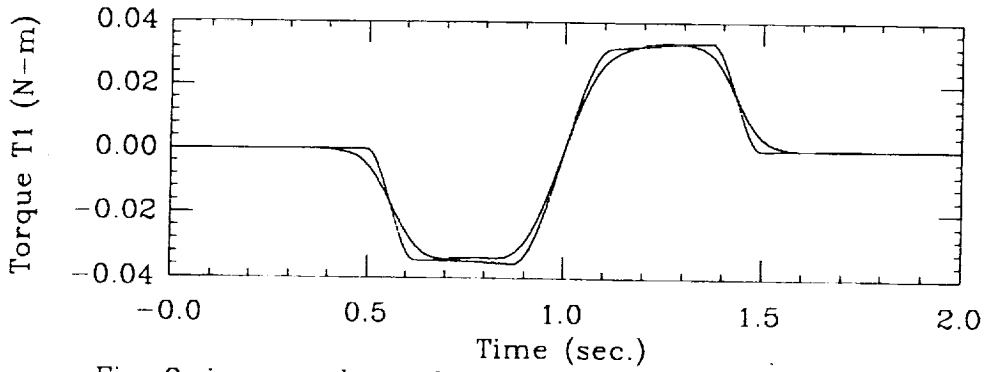


Fig. 9: inverse dynamics torque and rigid torque at joint 1

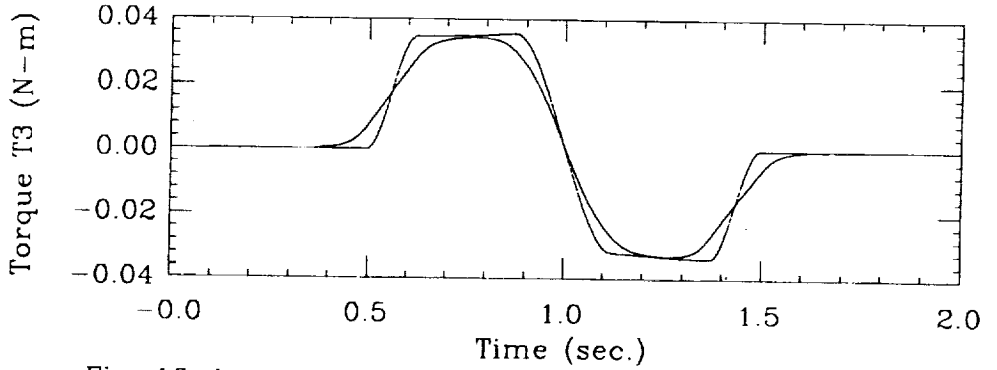


Fig. 10: inverse dynamics torque and rigid torque at joint 3

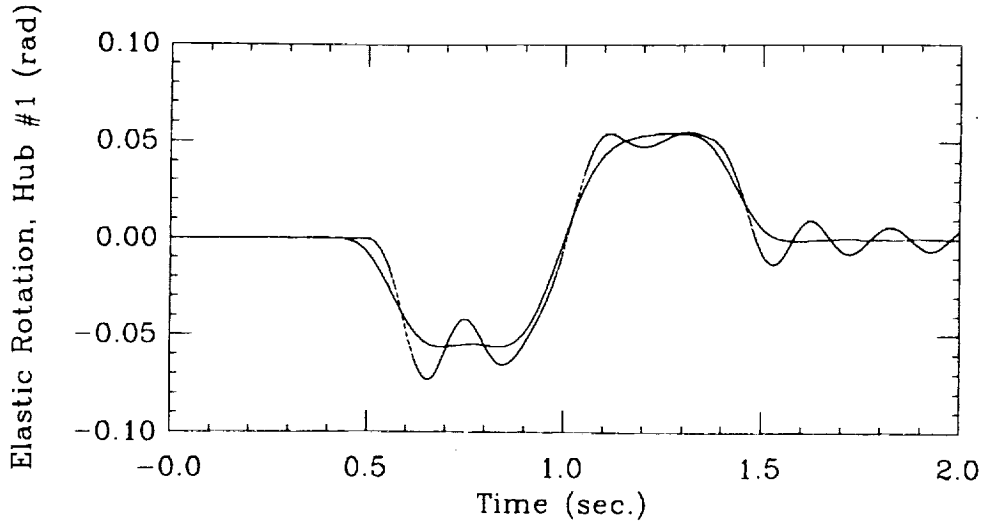


Fig. 11: elastic rotation: inverse dynamics vs. rigid torques

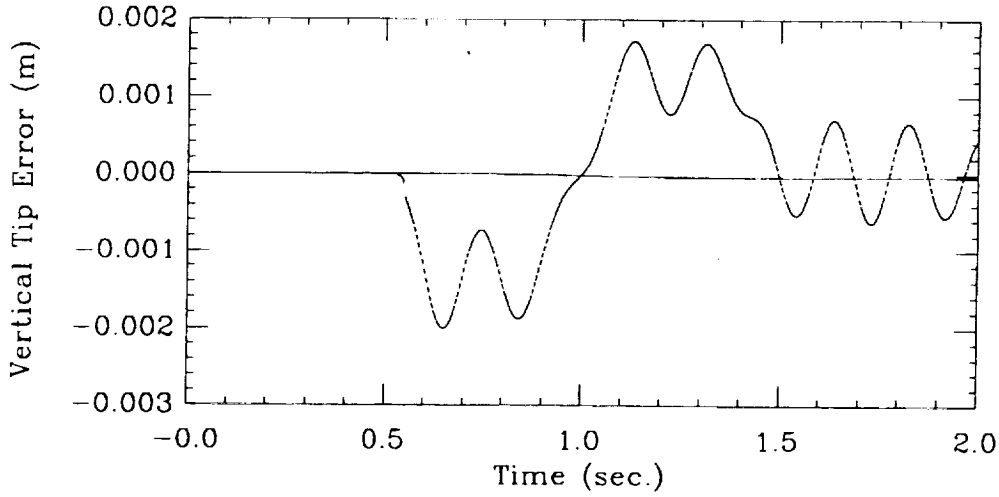


Fig. 12: vertical tip error: inverse dynamics vs. rigid torques